

Introduction

We investigate mixing layer height (MLH) estimates using long-term (2011-2019) observations from the Atmospheric Radiation Measurement (ARM) Southern Great Plains site. Various ground-based remote sensing retrievals of the MLH were evaluated in particular to assess the performance of ceilometer retrievals. Results showed the largest limitations during the afternoon MLH therefore, a retrieval to include the lifting condensation level (LCL) as an auxiliary measurement was implemented. Cloud typing and sky regimes are used to evaluate the retrieval performance by classifying different cloud conditions and radiative forcings that may influence the evolution of the mixed layer depth. This work will guide the improvement and identification of reliable MLH retrievals by including supplement observations of cloud properties, surface radiation, and near-surface thermodynamics.

Data and Methods

Daytime MLH at the Atmospheric Radiation Measurement Southern Great Plains (SGP) Site (36.607°N, 97.488°W)

Instrument	Data and Method	Dates
Doppler Wind Lidar (DWL)	PBLH Random Forest (RF) Method (Krishnamurthy et al. 2021)	2019
	PBLH Tucker Method (VAP) (Tucker et al. 2009)	
Vaisala CL31 ceilometer	Vaisala BL-View Software (Selection Method: Duncan et al. 2022) PBLH Haar Wavelet Method (Caicedo et al. 2020)	2011-2020
AERI Atmospheric Emitted Radiance Interferometer	PBLH Turner Method (Turner and Blumberg, 2019) Lifting Condensation Level (LCL)	04/2019 - 07/2019
Radiosonde	Radiosonde profiles and PBL VAP (Hefter, 1980 (Hefter); Liu and Liang, 2010 (LL); Seibert et al., 2000 and Sorenson et al. 1998 (BR5 and BR25))	2011-2020
	RADFLUX LCL Estimates (non VAP)	2011-2020

ARM SGP 2011-2020 Results

Radiosonde, doppler wind lidar (DWL), ceilometer, Atmospheric Emitted Radiance Interferometer (AERI), and Radiative Flux Analysis VAP (RADFLUX) data are used to evaluate MLH retrievals across remote sensing platforms.

All radiosonde methods showed large variability in MLHs through the study period (Figure 1). The Liu and Liang (2010) method was chosen as the validation data set.

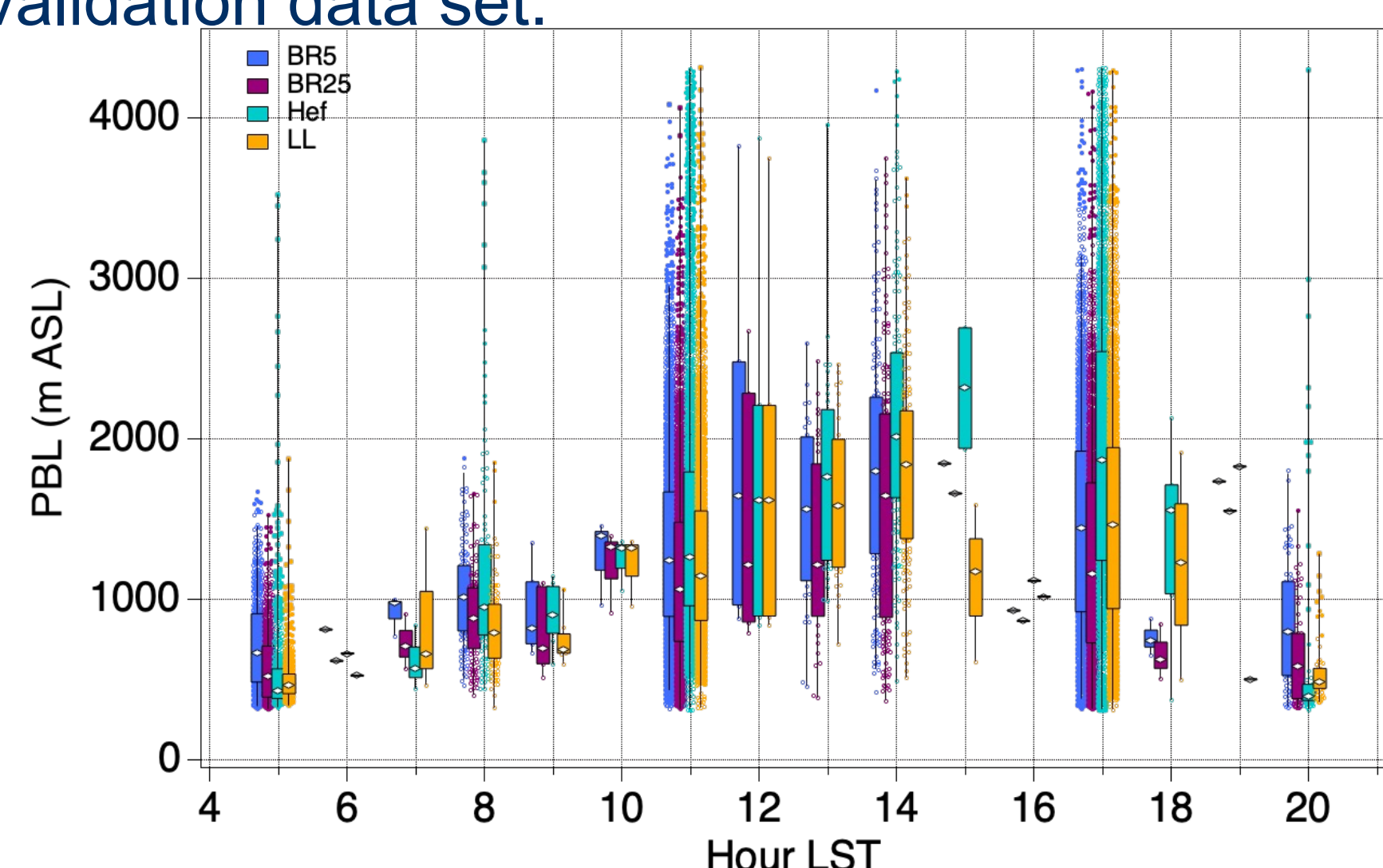


Figure 1 – ARM SGP Sondes retrievals for 2011-2020 displayed as a function of hour. ARM SGP PBLH VAP includes Hefter (Hef), Liu and Liang (LL), and Bulk Richardson methods with critical threshold 0.25 (BR25) and 0.5 (BR5). Box displays interquartile range with white \diamond markers depicting the median. Whiskers expand to the min and max of all data points. Circle markers show all data points with filled markers depicting outliers and square markers depicting far outliers.

- AERI retrievals showed the best correlation to radiosonde PBLHs, while the DWL RF method followed in second likely due to the RF training using LL sondes (Table 1).
- Although the ceilometer Haar wavelet algorithm showed an overall improved correlation to sonde PBLHs than Vaisala, the afternoon ML collapse was consistently not captured (Figure 2).

Table 1 – Linear regression fit of ceilometer, DWL, and AERI PBLH retrievals against radiosonde LL PBLHs

	r ²	Slope	Offset	RMSE (m)	Mean (m)	Mean Bias (LL - retrieval)
Haar Wavelet	0.42	0.60 ± 0.01	557.9 ± 14.8	1347.5	1220.2	-3.9
DLW RF	0.51	0.66 ± 0.01	610.0 ± 16	1237	1106.6	109.7
DWL Tucker	0.49	0.64 ± 0.01	603.3 ± 15.5	1352.5	1187.9	28.4
AERI	0.69	0.63 ± 0.03	311.9 ± 41.2	1336.6	1249.6	-33.3
Vaisala	0.26	0.61 ± 0.01	419.9 ± 20.3	964.1	938.2	278.1

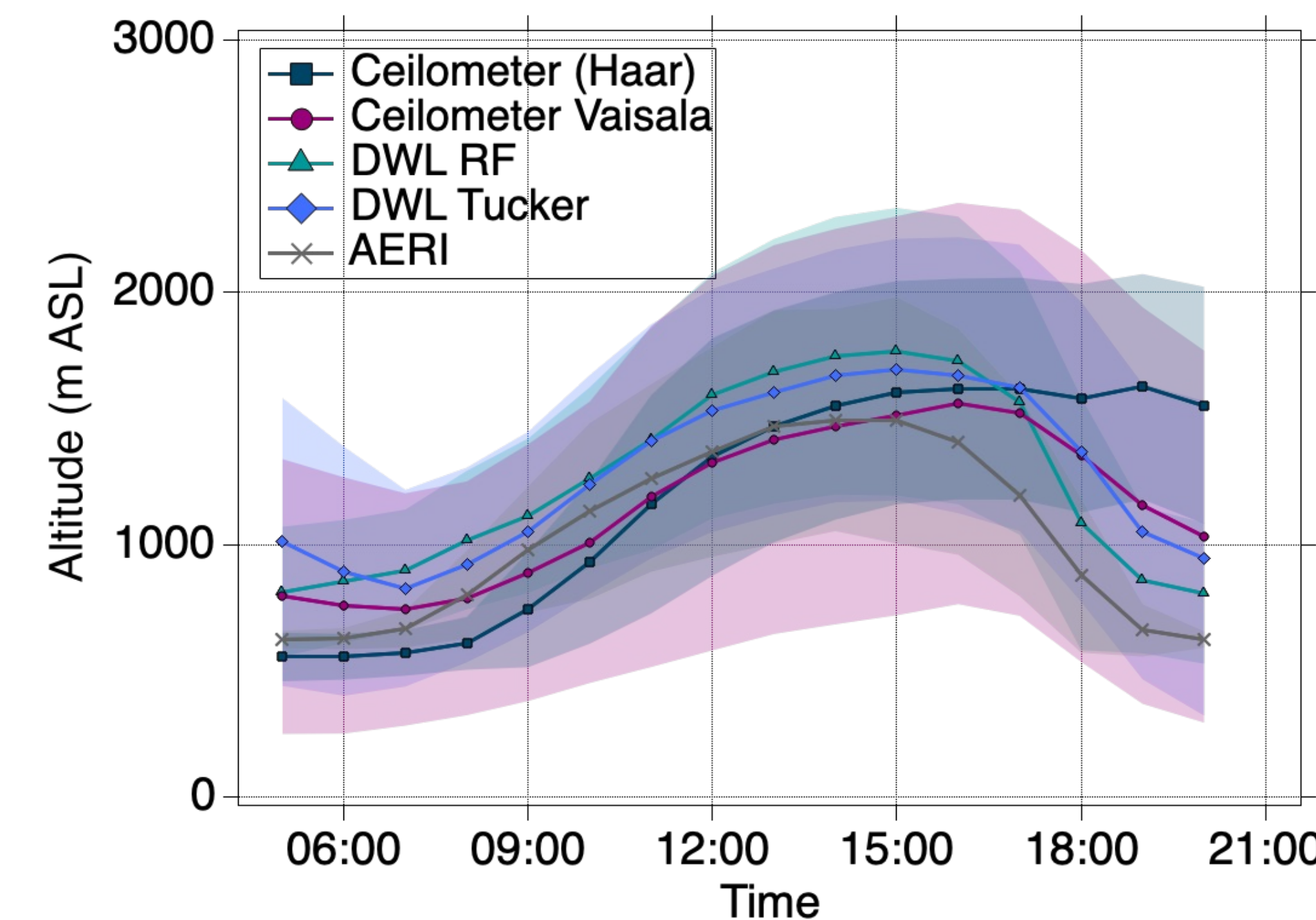


Figure 2 – Hourly diurnal averages in LST (April - July 2019)

Afternoon MLH Retrievals

Focus period of April 17, 2019 – July 31, 2019

- High temporal resolution of AERI PBL retrievals to evaluate the lack of afternoon collapse in ceilometer retrievals
- Caicedo et al., (2020) uses a continuation parameter to guide PBLH retrievals and prevent unrealistic jumps in retrievals by comparing to the last 30-minute moving average of PBLH retrievals. For the afternoon time period (sunset time - 3hrs to sunset time +1hr), the average LCL height was used instead of PBLH retrievals.
- LCL heights derived from both AERI and RADFLUX data were tested for the focus period (Figure 3). The use of RADFLUX LCL resulted in better agreement to LL retrievals than that of AERI LCL (Table 2).

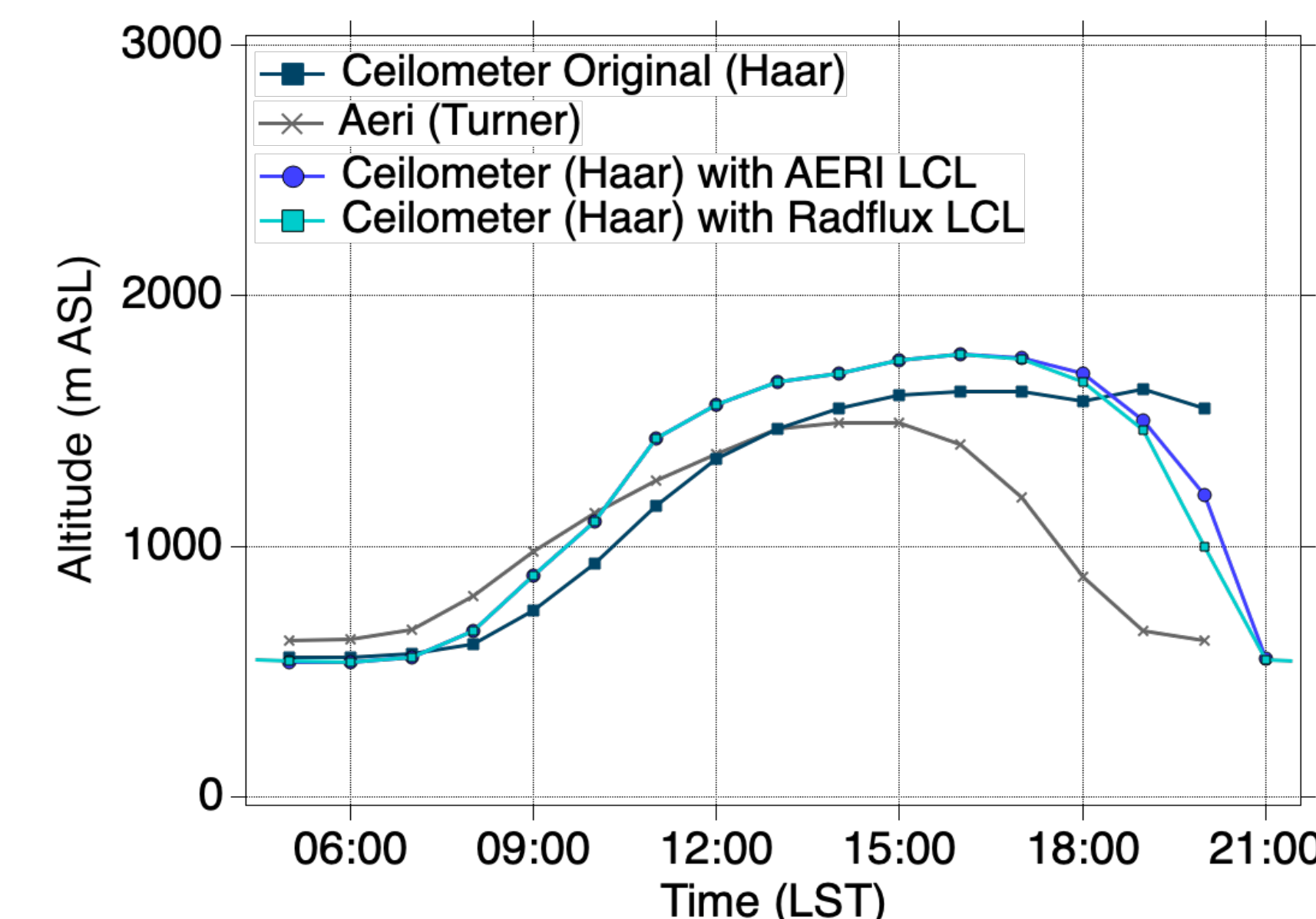


Figure 3 – Hourly diurnal averages (April - July 2019)

Table 2 – Ceilometer PBLH retrievals using RADFLUX and AERI derived LCL heights for afternoon collapse. Results are compared to both radiosonde and AERI-derived PBLHs.

	Radiosonde LL			AERI		
	r ²	Slope	Offset	r ²	Slope	Offset
LCL (AERI)	0.59	0.72 ± 0.03	407.2 ± 47.6	0.40	0.78 ± 0.02	415.5 ± 21.9
LCL (RADFLUX)	0.64	0.75 ± 0.03	338.9 ± 43.6	0.41	0.79 ± 0.02	396.9 ± 21.8

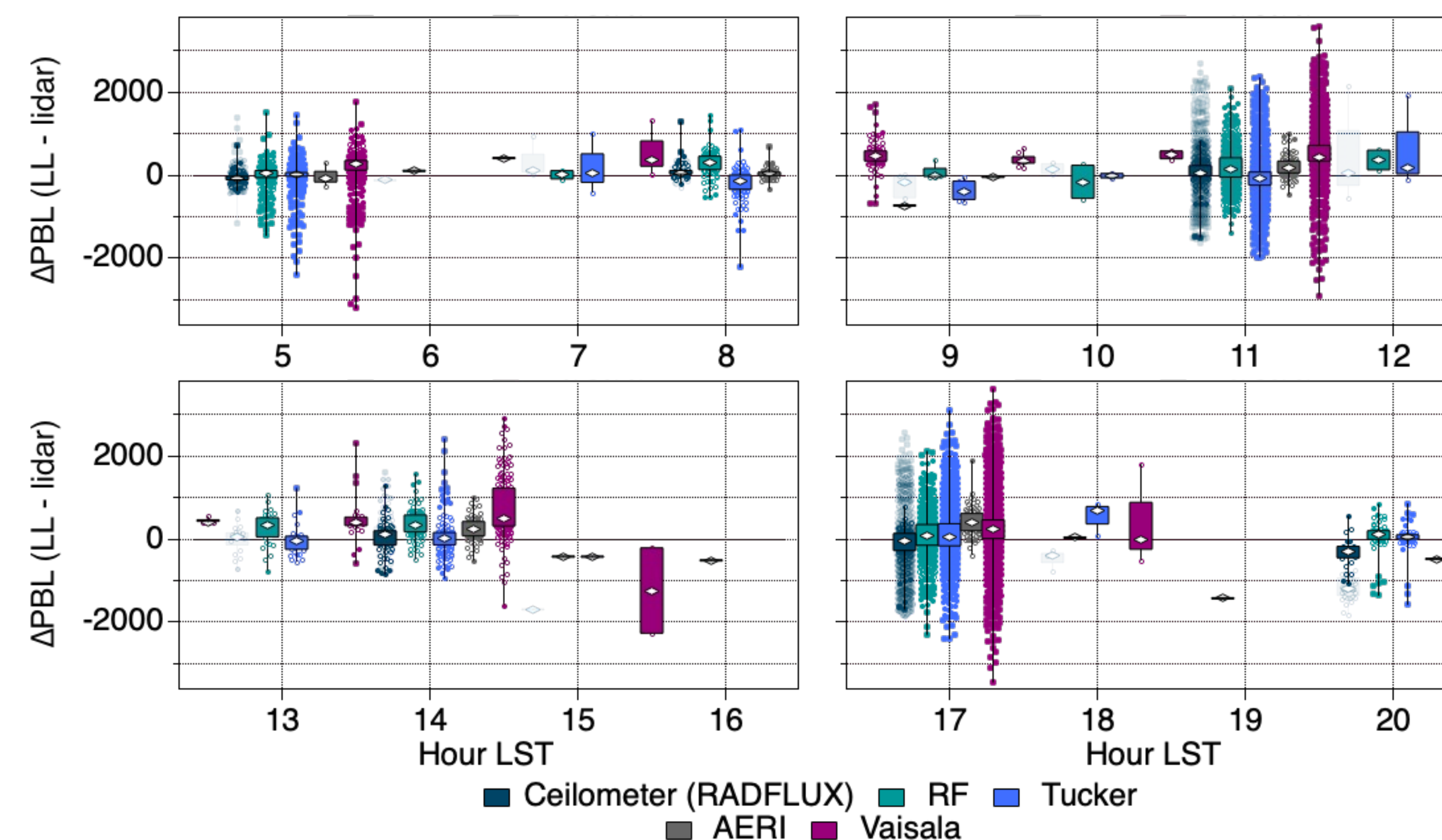


Figure 4 – Hourly statistical comparison of PBLHs from remote sensing instrumentation to the radiosonde LL retrieval for April - July 2019. Δ PBL is calculated for each data point as LL PBLH - lidar retrieval PBLH. All heights are compared with corresponding measurements in a 10-minute window (e.g. 10:10:00 - 10:19:59). Box displays interquartile range with white \diamond markers depicting the median. Whiskers expand to the min and max of all data points. Circle markers show all data points with filled markers depicting outliers and square markers depicting far outliers.

Cloud and Sky Regimes

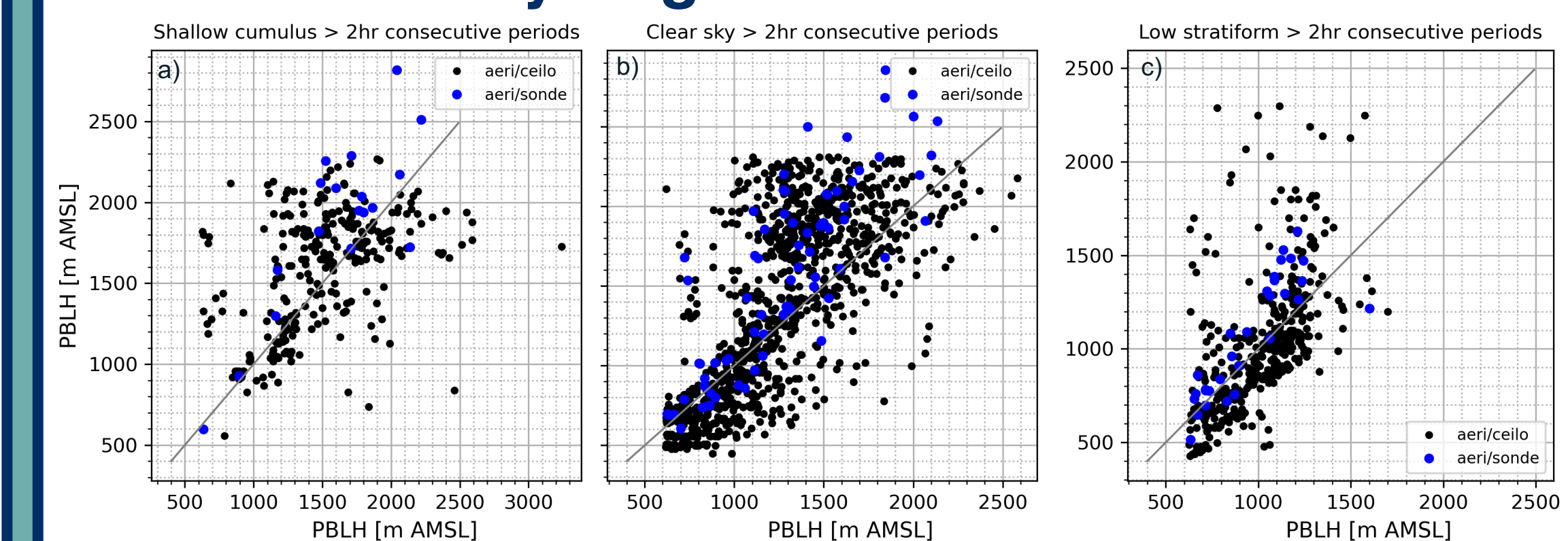


Figure 5 – Comparison of ceilometer retrievals using LCL heights and AERI PBLHs retrievals in black and comparison of AERI and radiosonde LL retrievals in blue during a) shallow cumulus, b) clear sky, and c) low stratiform regimes. A cloud type period of at least 2 hours in duration was required when classifying retrievals.

- Sedlar et al. (2021) cloud regime algorithm was used to evaluate MLH retrievals during shallow cumulus, low stratiform, and clear sky conditions.
- Results showed good agreement between ceilometer and AERI retrievals particularly during shallow cumulus, and similar mean bias errors (MBE) and RMSE.

		Shallow Cumulus	Clear Sky	Low Stratiform
Ceilometer	MBE	8 m	78 m	122 m
	RMSE	292 m	413 m	404 m
AERI	MBE	114 m	265 m	284 m
	RMSE	206 m	396 m	441 m

Summary and Future Work

- Radiosonde MLH retrieval methods showed a large spread revealing large limitations in sonde retrievals.
- Ceilometer retrievals using the Haar Wavelet algorithm showed significant improvement compared to the Vaisala software.
- Afternoon collapse showed the largest limitation of the Haar Wavelet algorithm but the use the LCL height significantly improved estimations of the MLH.
- Shallow cumulus cloud regime showed the best agreement between retrievals (note No. comparison points). Overall, AERI and ceilometer comparisons showed similar MBE and RMSE.
- Future work will use measurements from the NOAA GML SURFRAD Network combining ceilometer profiles, cloud, and radiation data sets into a random forest algorithm.

References

Caicedo, V., Delgado, R., Sakai, R., Knepp, T., Williams, D., Cavender, K., Lefer, B., & Szykman, J. (2020). An automated common algorithm for planetary boundary layer retrievals using aerosol lidars in support of the u.s. epa photochemical assessment monitoring stations program. *Journal of Atmospheric and Oceanic Technology*, 37(10), 1847–1864. <https://doi.org/10.1175/JTECH-D-20-0050.1>

Duncan, J. B., Bianco, L., Adler, B., Bell, T., Djalalova, I. v., Riihimaki, L., Sedlar, J., Smith, E. N., Turner, D. D., Wagner, T. J., & Wilczak, J. M. (2022). Evaluating convective planetary boundary layer height estimations resolved by both active and passive remote sensing instruments during the CHEESEHEAD19 field campaign. *Atmospheric Measurement Techniques*, 15(8), 2479–2502. <https://doi.org/10.5194/amt-15-2479-2022>

Krishnamurthy, R., Newsom, R. K., Berg, L. K., Xiao, H., Ma, P. L., & Turner, D. D. (2021). On the estimation of boundary layer heights: A machine learning approach. *Atmospheric Measurement Techniques*, 14(6), 4403–4424. <https://doi.org/10.5194/amt-14-4403-2021>

Liu, S., & Liang, X. Z. (2010). Observed Diurnal Cycle Climatology of Planetary Boundary Layer Height. *Journal of Climate*, 23(21), 5790–5809. <https://doi.org/10.1175/2010JCLI3552.1>

Sedlar, J., Riihimaki, L. D., Lantz, K., & Turner, D. D. (2021). Development of a Random-Forest Cloud-Regime Classification Model Based on Surface Radiation and Cloud Products. *Journal of Applied Meteorology and Climatology*, 60(4), 477–491. <https://doi.org/10.1175/JAMC-D-20-0153.1>

Tucker, S. C., Brewer, W. A., Banta, R. M., Senff, C. J., Sandberg, S. P., Law, D. C., Weickmann, A. M., & Hardesty, R. M. (2009). Doppler Lidar Estimation of Mixing Height Using Turbulence, Shear, and Aerosol Profiles. *Journal of Atmospheric and Oceanic Technology*, 26(4), 673–688. <https://doi.org/10.1175/2008JTECHA1157.1>

Turner, D. D., & Blumberg, W. G. (2019). Improvements to the AERtoe thermodynamic profile retrieval algorithm. *IEEE Journal of Selected Topics in Applied Earth Observations and Remote Sensing*, 12(5), 1339–1354. <https://doi.org/10.1109/JSTARS.2018.2874968>